Representation of the QBO in the Tropical Stratospheric Wind by Nonlinear Principal Component Analysis

January 15, 2002

Kevin Hamilton
Department of Meteorology
and International Pacific Research Center
University of Hawaii at Manoa
Honolulu, Hawaii 96822
kph@soest.hawaii.edu

William W. Hsieh
Department of Earth and Ocean Sciences
University of British Columbia
Vancouver, B.C. V6T 1Z4
Canada

Abstract

The zonal winds at several levels between 70 and 10 hPa (roughly 20-30 km) measured at near-equatorial stations during 1956-2000 were analyzed to produce a one-dimensional approximation. The neural network-based technique applied was the circular nonlinear principal component analysis (NLPCA.cir) designed to characterize quasi-periodic phenomena. The reconstructed height-time series of wind based on the one-dimensional NLPCA.cir captures many of the characteristic features of the observed quasi-biennial oscillation (QBO). The nonlinear results were evaluated relative to comparable linear principal component analysis and found to produce a superior one-dimensional representation of the data. The NLPCA.cir analysis produces a single time series of QBO phase based on data at all levels. This phase was then applied to demonstrate a strong correlation of the state of the tropical QBO and boreal winter high-latitude stratospheric temperatures.

1 Introduction

The prevailing winds in the equatorial stratosphere are observed to undergo an oscillation between strong westerly (i.e. eastward) and easterly (i.e. westward) winds, with the transition from one phase to the other occurring roughly every year. This quasi-biennial oscillation (QBO) of the circulation dominates any annual cycle or other variations in the low-latitude stratosphere [see *Hamilton*, 1998a, and *Baldwin et al.*, 2001, for recent reviews]. The period of the oscillation has been observed to vary from cycle to cycle between roughly 22 and 33 months, but the mean period over the last half-century of observations is close to 28 months. The variability of the period and the fact that the mean period appears to be incommensurate with the annual cycle or any harmonics or subharmonics of the annual cycle indicates that the QBO is driven primarily by the internal fluid mechanics of the atmosphere. Thus it is to be strongly contrasted with the familiar astronomically-driven oscillations (seasonal cycle, tides) which are genuinely periodic. However, the stratospheric QBO is much more regular than other extensively-studied oscillatory phenomena in the atmosphere (such as the Southern Oscillation or North Atlantic Oscillation).

The nearly-periodic, but somewhat irregular, behavior makes the QBO one of the most intriguing phenomena in geophysics. A standard height-time record of monthly-mean zonal wind constructed from balloon observations up to 10 hPa ($\sim$30 km) at near-equatorial stations has been carefully updated over the years [*Wallace*, 1973; *Coy*, 1979; *Naujokat*, 1986; *Marquardt and Naujokat*, 1997] and has become a familiar and widely-analyzed data record. Among the characteristic properties that have been clearly documented in these data are: *i*) consistently downward phase propagation of wind reversals, *ii*) a strong tendency for the wind accelerations at any level to be concentrated into limited periods near the wind reversals (leading to a roughly square-wave appearance to the time series at any particular level), *iii*) a corresponding tendency for the reversals to be associated with the downward passage of strong vertical shear zones, *iv*) asymmetry between the wind reversals such that the easterly-to-westerly transition is more rapid than the westerly-to-easterly transition (and the peak westerly shear is stronger than the peak easterly shear), and *v*) fairly regular downward propagation of the westerly transition, but a tendency found in many cycles for the easterly transition to "stall" for several months between about 30 and 50 hPa (this effect accounts for much of the period variability from cycle to cycle).

The somewhat complicated vertical structure of the QBO in zonal wind makes it difficult to characterize the "phase of the QBO" in a completely adequate way. The equatorial QBO is known to be correlated with a number of important aspects of atmospheric behavior such as high-latitude stratospheric circulation [e.g. *Holton and Tan*, 1980, 1982; *Dunkerton and Baldwin*, 1991; *Baldwin and Dunkerton*, 1998], the distribution of stratospheric ozone and other trace constituents [e.g., *Tung and Yang*, 1994; *Randel et al.*, 1998], and may be connected with such features of tropospheric climate as the Southern Oscillation [e.g. *Xu*, 1992; *Gray et al.*, 1992, *Geller et al.*, 1997] and even the frequency of occurrence of tropical cyclones

[*Gray*, 1984]. These connections have generally been studied by using the zonal wind at one arbitrarily-chosen level to characterize the phase of the QBO, but for many applications a quantity that could characterize the whole vertical structure at a given time would be more relevant. Simplified statistical representations of the QBO wind variations could also be useful in characterizing the modest annual cycle effects apparent in the observed record, and for comparison of observed QBO with corresponding features seen in comprehensive general circulation model (GCM) simulations [e.g., *Takahashi*, 1996, 1999; *Horinouchi and Yoden*, 1998; *Hamilton et al.*, 1999, 2001]. Finally, recent work of *Salby and Callaghan* [2000] suggests that the period of the stratospheric QBO may be modulated by the 11-year solar activity cycle. As *Salby and Callaghan* noted, such a modulation would have significant implications for understanding and predicting solar effects on the global climate system. Again *Salby and Callaghan* performed their analysis using a QBO period estimated by using winds at a single level. A characterization of the QBO phase evolution that used wind information over a deeper layer might be more meaningful.

There have been some more sophisticated efforts to obtain a time-series representation of the phase of the equatorial zonal wind QBO (along with an associated characteristic vertical structure). In particular, *Wallace et al.* [1993] computed the first two principal components (PCs) of the height-time section and found that the time series of the coefficients were quasi-cyclic and in quadrature, allowing the phase of the QBO to be characterized by the arctangent of the ratio of the coefficients. *Fraedrich et al.* [1993] and *Wang et al.* [1995] examined the problem via the singular spectrum analysis (often referred to as extended PC analysis) using a window of 40 months. They also found that the leading two extended PCs were in quadrature and described a steadily descending oscillation.

Unfortunately, the leading PCs or extended PCs describe only the crudest aspects of the zonal wind QBO and miss many details characteristic of the actual observations. Notably the leading PCs (or extended PCs) tend to describe a near-sinusoidal oscillation rather than the more square-wave behavior apparent in the real QBO. Also the first modes in the PC and extended-PC approaches capture virtually none of the asymmetry between westerly and easterly shear zones (and westerly and easterly acceleration regimes) that is such a prominent characteristic of the observations (in every QBO cycle observed so far).

The limitation of the leading PCs (or extended PCs) as descriptions of the full QBO is not surprising, as the PCs are just linear least-squares fits to the data. Recently nonlinear generalizations of the PC approach using neural network techniques have been developed and applied to the analysis of geophysical phenomena such as the El Niño-Southern Oscillation [*Monahan*, 2001; *Hsieh*, 2001; *Hsieh and Wu*, 2002]. The present paper will apply the nonlinear principal component analysis (NLPCA) to the observed equatorial stratospheric wind record. The rich detail characteristic of each observed QBO cycle, along with the slightly irregular cycle-to-cycle nature of the QBO, make this a particularly appealing phenomenon for application of the NLPCA technique. The present analysis will show that the nonlinear approach leads to a significantly more complete characterization of the QBO behavior in a single time series, than does the comparable linear analysis.

2 Data

The data analyzed here were obtained from Barbara Naujokat of the Free University of Berlin and are monthly means of the zonal wind component measured by twice-per-day balloon ascents at: Canton Island (2.8^{o}N) during January 1956 through August 1967, Gan (0.7^{o}S) from September 1967 through December 1975, and Singapore (1.4^{o}N) from January 1976 through December 2000. This represents a continuation of the data record analyzed in *Naujokat*, [1986], *Wallace et al.*, [1993], *Fraedrich et al.*, [1993], *Wang et al.,* [1995], and in many other studies. Values at 70, 50, 40, 30, 20, 15 and 10 hPa (i.e. from about 20 km to 30 km altitude) are used. A plot of a slightly smoothed version of the monthly data (with 45-year mean value at each level removed) for 20 years is shown in Fig. 7b below.

3 Brief Description of the NLPCA.cir Method

In principal component analysis (PCA), also known as empirical orthogonal function analysis, a straight line approximation to the dataset is sought which accounts for the maximum amount of variance in the data. There are now several types of neural network (NN) models which use, instead of the straight line, a continuous curve to approximate the data. Using a multi-layer perceptron NN formulation, the nonlinear PCA (NLPCA) method of *Kramer* [1991] is capable of finding an open curve to approximate the data. However, for periodic or quasi-periodic phenomena, it would be more appropriate to fit the data with a closed curve. *Kirby and Miranda* [1996] introduced an NLPCA with a circular node at the bottleneck (henceforth NLPCA.cir), capable of extracting closed curve solutions. Applications to the tropical Pacific climate variability have been made with the NLPCA by *Monahan* [2001] and *Hsieh* [2001], and with the NLPCA.cir by *Hsieh* [2001].

The NLPCA.cir used here is described in detail in *Hsieh* [2001]. The input data are in the form $\mathbf{x}(t) = [x_1, \ldots, x_l]$, where each variable $x_i, (i = 1, \ldots, l)$, is a time series containing n observations. The information is mapped forward through a bottleneck to the output $\mathbf{x}'$ (Fig. 1). The parameters of the network are solved by minimizing the cost function, which is basically the mean square error (MSE) of $\mathbf{x}'$ relative to $\mathbf{x}$. Because of local minima in the cost function, an ensemble of 30 NNs with random initial weights and bias parameters was run. Also, 20% of the data was randomly selected as test data and withheld from the training of the NNs. Runs where the MSE was larger for the test dataset than for the training dataset were rejected to avoid overfitted solutions. Then the NN with the smallest MSE was selected as the solution. As noted in *Hsieh* [2001], the NLPCA.cir can be set up in a general or a restricted configuration, where in the general configuration, the solution can be either an open or a closed curve, while the restricted configuration favors a closed curve. In this study, the general configuration will be used.

4 Analysis of the Equatorial Wind Data by NLPCA.cir

For this analysis the wind values at each of the 7 vertical levels had the 45-year mean removed (but the weak seasonal cycle was retained). These zonal wind values are then the 7 inputs into the NLPCA.cir (Fig. 1), with m, the number of hidden neurons in the encoding layer (and in the decoding layer) varying from 2 to 8. No weight penalty [*Hsieh*, 2001] was needed in the cost function as the signal to noise ratio was very good. Table 1 gives the root mean square error (RMSE) as a function of m. Beyond m=6 the decrease in RMSE obtained by increasing the hidden layers is very slow, so the $m = 6$ solution is chosen as the most appropriate one.

The NLPCA.cir mode 1 solution gives a closed curve in a 7-dimensional space. The system goes around the closed curve once, as the NLPC θ varies through one cycle. Fig. 2 shows the solution in 3 of the 7 dimensions, namely the wind anomalies at 10, 30 and 70 hPa. The NLPCA.cir mode 1 explains 94.8% of the variance. For comparison, the linear PCA yields 7 modes explaining 57.8, 35.4, 3.1, 2.1, 0.8, 0.5 and 0.3% of the variance, respectively. Thus the variance explained by the NLPCA.cir mode 1 (94.8%) exceeds the variance explained by PCA 1 and 2 combined (93.2%). The PCA mode 1 is also shown as a straight line in Fig. 2. The MSE of NLPCA.cir mode 1 is only 0.12 that of the PCA mode 1, indicating a much better fit to the data by the nonlinear mode.

To provide the most appropriate linear approach for comparison with the NLPCA.cir, the time series for the first two linear PCAs were divided by their standard deviation and a phase angle then defined as the arctangent of the ratio of the two normalized PCA coefficients. This was then used as the basis for a one-parameter linear "circular" approximation. This linear model accounts for 83.0% of the variance in the zonal wind time series, vs. the 94.8% from the first NLPCA.cir mode.

The time series for the nonlinear principal component (NLPC) θ is shown in Fig. 3 for $m =$ 2, 4, 6 and 8. The results are rather similar for all these values of m, demonstrating the stability

of the NLPC approach in this case. The NLPC completes slightly more than 19 cycles over the 45 years considered, for an average period of about 28 months. The NLPCA.cir representation of a single QBO cycle as a function of θ is given in Fig. 4. However, Fig. 3 shows that θ does not advance uniformly with time through the QBO cycle (note, for example, the conspicuous slowing down of θ progression around 0.7-0.9). To quantify this effect, all the monthly θ values for 1956-2000 were binned into 20 equal θ intervals. The resulting histogram (not shown) has a variation of between 3 and 58 monthly values within the individual bins, confirming the impression in Fig. 3 that θ consistently advances through some values quickly and through other values slowly. After applying a 3-point running mean to the histogram function, the QBO cycle of Fig. 4 was replotted with respect to θ_{weighted}, which is θ weighted by the smoothed histogram distribution (Fig. 5). The purpose of this weighting is to produce an independent variable that equally distributes the time the QBO spends in any range. This gives a more accurate picture of how the QBO typically progresses with time over one cycle, and can be regarded as an objectively determined "composite" QBO cycle using the NLPCA.cir approach. Earlier attempts to construct composite QBO cycles [e.g. *Naujokat*, 1986; *Baldwin et al.* 2001] were made with the standard "superposed epoch" approach. These earlier composites tended to smooth out some of the features seen consistently in every QBO cycle, notably the strength of the shear zones, and the asymmetry in phase progression and shear strength between the descending easterly and westerly regimes. The present NLPCA.cir "composite" in Fig. 5 does a much better job of capturing these subtleties, including the tendency for the descending easterly phase to "stall" between 30 and 50 hPa. The equivalent of Fig. 5 was computed using the one-parameter linear circular approximation and is shown here as Fig. 6. This is much less able than the NLPCA.cir treatment to capture the characteristic irregularities in QBO wind regime propagation.

The NLPCA.cir reconstructed component (NLRC1) was calculated; this represents the approximation of the original 7 time series (at the 7 vertical levels) by the single NLPCA.cir. The reconstructed time series from linear PCA mode 1 (RC1), and from PCA modes 1 and 2 (RC1+2) were also calculated. The correlation and root mean square error (RMSE) between these reconstructed time series and the observations are given in Table 2. The NLRC1 and RC1+2 are plotted for the period 1981-2000 in Fig. 7, together with the raw observations. Reconstructions using additional linear PCA modes will, of course, fit the observations better, but will also be fitting to the noise in the data. Here RC1+2 is already more noisy in appearance than NLRC1. The single RC1 is less noisy than RC1+2, but models the actual data rather poorly, particularly around 30-50 hPa (Table 2). The single parameter NLPCA.cir reconstruction is better correlated with the observations and has a lower MSE than the two-mode RC1+2 reconstruction. Inspection of Fig. 7 shows that the NLRC1 reconstruction captures much better the strong shear zones and rapid accelerations apparent in the raw data than does the RC1+2.

A number of earlier studies have addressed the possible role of the annual cycle in the dynamics of the QBO (e.g., Dunkerton, 1983b, 1990). Wallace et al. (1993) found that their QBO phase angle defined from the first two linear PCAs, on average, advanced most rapidly in April-May and least rapidly in December-January. Fig. 8 shows the present NLPCA.cir θ plotted each month for the first 15 consecutive years of the record. The tendency for the phase to advance most rapidly in boreal spring is evident in almost all individual years. Fig. 9 shows the phase difference between successive months averaged over all years of data for each pair of adjacent calendar months. On average the phase varies almost three times as much between May and June as between September and October. This shows a clear dependence of the QBO behavior on season. The rapid phase variation in boreal spring found here is consistent with the earlier study of Wallace et al. However, Fig. 9 has a more semiannual nature than the comparable result from Wallace et al., with a secondary maximum appearing in Fig. 9 in November-December.

The possibility that the QBO period may be subject to some systematic low-frequency modulation was studied originally by *Quiroz*, [1981] and *Dunkerton and Delisi*, [1985]. As noted in the Introduction, the recent work of *Salby and Callaghan*, [2000], has revived interest

in this possibility. Earlier studies have all used a simple characterization of QBO period in terms of the zero-crossings of the observed wind at a particular level (generally near 50 hPa). The present objective determination of the phase of the QBO, using data from all the levels, allows this issue to be revisited. A "local" period of the QBO was defined for each month proportional to the reciprocal of the rate of phase change, $\Delta\theta_{weighted}/\Delta t$. The monthly values defined this way are rather noisy, so Fig. 10 shows the reciprocal of the 28-month running mean of $\Delta\theta_{weighted}/\Delta t$. There does seem to be a systematic modulation with the longest periods occurring in the mid to late 1960s, and the mid to late 1980s, while the shortest periods occurred around 1960, the early 1970s and the late 1990s. The reason for such systematic modulation of the QBO period is not known, although possibilities that have been suggested include: variations in volcanic aerosol loading or concentrations of other radiatively-active constituents in the stratosphere [*Dunkerton*, 1983a], variations in tropospheric climate leading to modulation of the waves thought to force the QBO wind accelerations [*Geller et al.*, 1997], or solar cycle variations [*Salby and Callaghan,*, 2000]. The present results in Fig. 10 do not seem to show any clear connection with the 11-year solar cycle. The results in the present Fig. 10 differ to some extent from earlier time series of QBO periods deduced from simple inspection of zero-crossings of the time series at 30 hPa (Geller et al., 1997) or 50 hPa (Salby and Callaghan, 2000). Features in common in all three studies include a clear lengthening of the period for a 8-10 year era centered around 1966 and an era of very short periods in the early 1970's. The analyzed variations in QBO period during the 1980's and 1990's are somewhat different among the three studies, with the 50 hPa estimates of Salby and Callaghan showing a strong maximum centered around 1986 and a deep minimum in the early 1990's, which do not have clear counterparts in the present results or those of Geller et al.

5 Application of NLPCA.cir-based QBO Phase to Study Extratropical Stratospheric Effects

The phase of the tropical QBO is known to be correlated with the extratropical stratospheric circulation, a fact first demonstrated by *Holton and Tan*, [1980, 1982] and now often referred to as the "Holton-Tan (HT) effect". In particular, HT and later investigators have shown that the polar stratosphere during NH winter is on average warmer, and the westerly vortex circulation is weaker, when the zonal-mean zonal winds at the equator near 40 hPa are easterly than when they are westerly. The HT effect is strongest in November-January and is virtually absent later in the winter. This effect has a plausible physical explanation in terms of the expected modulation of quasi-stationary planetary wave propagation by the mean flow and has been reproduced in various models of the stratospheric circulation including sophisticated GCMs [*Hamilton*, 1998b; *Takahashi*, 1999].

The HT effect has generally been studied using the equatorial wind at a single level near 40 hPa to characterize the QBO phase (the 40 hPa level is chosen as this generally is found to maximize correlations with the indicators of extratropical circulation). Physically there is no reason to expect that the winds at any particular level will control the planetary wave modulation. Thus it is of interest to revisit the HT effect with the present NLPCA.cir characterization of the tropical QBO phase.

The January-mean North Pole (NP) 30 hPa temperatures from the NCEP/NCAR reanalyses for the 42-year period 1958-1999 were used to characterize the extratropical winter stratosphere. Then 42 separate (but overlapping) θ ranges were defined so that each contained exactly 21 of the θ values from the NLPCA.cir analysis for these 42 Januaries. For each of these θ ranges the quantity ΔT was computed as the NP temperatures averaged over the 21 Januaries within the range minus that averaged over the 21 Januaries out of the range. The largest ΔT of 5.4^oC was obtained for a θ range between -0.86675 and 0.44775. This θ range then is the analogue of the "easterly QBO phase" as defined using the raw wind value at one level by HT and others. Inspection of Fig. 4 shows that this range of θ corresponds almost exactly to the period of anomalously easterly wind at 40 hPa in the composite QBO cycle.

The first column in Table 3 shows the phases for each January defined by this NLPCA.cir criterion. The second column shows the anomaly in the raw equatorial wind time series at 40 hPa. There is general agreement between the two measures of QBO phase, but there are some years where there are differences. For example, January 1968 emerges as "easterly" by the NLPCA.cir definition but the 40 hPa winds are anomalously westerly, and similarly in January 1995 the 40 hPa winds are westerly, but the NLPCA.cir definition is "easterly". If the ΔT is computed using the average NP temperatures in the 21 Januaries with most easterly 40 hPa wind minus the average during the 21 most westerly months (essentially following the original HT approach), then a value of 4.0^oC is obtained. This suggests that the NLPCA.cir criterion may be better able to characterize the aspect of the tropical QBO that correlates with extratropical NH winter circulation. Another approach based on the linear PCs was also investigated. An angle was defined as the arctangent of the ratio of the amplitude coefficients of the first two linear PCs. The analysis described for the NLPCA.cir θ and NP temperature was repeated using this angle. The largest ΔT obtained is 4.2^oC. The phase characterization for each January using this procedure is shown in the final column of Table 3. It turns out that this linear PC approach yields identical results to the NLPCA.cir approach in 40 of the 42 years, the exceptions being 1995 and 1996. The situation in January 1995 is particularly interesting. The linear PC approach classifies this as westerly and the January-mean 40 hPa winds are in fact westerly. However, the 40 hPa winds in January represent something of a one month spike, with the value dropping over February and March, and the sustained westerly phase at 40 hPa beginning in April (see Fig. 7b). The NLPCA criterion classifies January 1995 as the end of an easterly phase while the linear PC approach classifies this month as the beginning of a westerly phase. As noted earlier, the NLPCA.cir phase determination for these two Januaries is "better" in the sense that it leads to an enhanced contrast in the average easterly vs. westerly NP temperature (5.2^oC vs. 4.2^oC). The statistical significance of the temperature differences was evaluated by comparing to 1000 values computed based on randomly selected sets of 21 years. The 5.2^oC threshold was exceeded by only 9 of 1000 of these random cases, while the 4.2^oC threshold was exceeded by 37 cases. So both approaches lead to results that are 95% significant.

6 Conclusion

Many geophysical data sets take the form of time series observations simultaneously at several spatial locations. In such cases it is often desirable to construct low-dimensional approximate representations of the full data set, hence the immense popularity of linear PC analysis. Ideally such an approximation should fit the individual data values accurately, and in such a way that the basic phenomena are preserved while what may be regarded as noise is minimized. Linear PC analysis is a computationally and conceptually straightforward approach, but it represents just one of many possible approximations that can be used. The results in this paper have shown that application of the NN-based, circular bottleneck NLPCA.cir approach described by *Hsieh* [2001] produces a one-dimensional approximation to the observed height-time variability of the equatorial stratospheric zonal winds with many desirable features. A single NLPC fits the data more accurately in terms of MSE than a comparable one-parameter linear fit or even the sum of the first two linear PCs. The reconstructed wind field with the single NLPC also shows less apparent noise than the linear PC reconstruction, and better captures some of the important characteristics of the observed QBO wind variations. The NLPC was used to construct a "typical" QBO cycle in the winds (Fig. 5) which captures such features as the very strong shear zones and westerly vs. easterly asymmetries better than comparable "composite" QBO cycles that have been constructed using linear approaches. The present typical QBO cycle determined from observations could serve as a useful comparison for a similar analysis of model simulated winds. The NLPC can also be used to study the time-varying modulation in QBO period in a way that uses the observations from all levels simultaneously, in contrast to earlier single-level approaches. Finally, the NLPCA.cir can also serve as the basis to study

how the equatorial QBO phase correlates with other aspects of the atmospheric circulation. In this paper it was shown that a stratification of NP 30 hPa January temperature data based on the NLPCA.cir-determined QBO phase resulted in isolation of a stronger QBO-related effect than that obtained using characterization of the QBO phase by either the single level or linear PCA-based approaches.

The stratospheric QBO is a good candidate for application of the NLPCA.cir approach, as it is clearly a quasi-periodic variation with subtle characteristic features in each cycle, but one with considerable irregularity in its phase progression. The NLPCA.cir as described here would be less useful for quasi-periodic variations with large modulations in amplitude, and the method would need to be modified to deal with such a case. The NLPCA.cir can be extended in other ways as well. Hsieh and Wu (2002) have developed the NLPCA analogue of linear singular spectrum analysis (also referred to as extended empirical orthogonal function analysis), and the present authors have now applied this technique to analysis of the stratospheric QBO (W.W. Hsieh and K. Hamilton, Nonlinear singular spectrum analysis of the tropical stratospheric wind, submitted to *Quarterly Journal of the Royal Meteorological Society*).

Acknowledgments

W. Hsieh was supported by research and strategic grants from the Natural Sciences and Engineering Research Council of Canada. The International Pacific Research Center is supported in part by the Frontier Research System for Global Change. The authors thank Barbara Naujokat for supplying the wind data. The authors also acknowledge the helpful comments of the two official reviewers.

References

Baldwin, M. and T.J. Dunkerton, Quasi-biennial modulation of the Southern Hemisphere stratospheric polar vortex. *Geophys. Res. Lett., 25*, 3343-3346, 1998.

Baldwin, M., L. Gray, T. Dunkerton, K. Hamilton, P. Haynes, W. Randel, J. Holton, M. Alexander, I Hirota, T. Horinouchi, D. Jones, J. Kinnersley, C. Marquardt, K. Sato and M. Takahashi, The Quasi-biennial oscillation. *Rev. Geophys., 39*, 179-229, 2001.

Coy, L., An unusually large westerly amplitude of the quasi-biennial oscillation. *J. Atmos. Sci., 36*, 174-176, 1979.

Dunkerton, T.J., Modification of stratospheric circulation by trace constituent changes. *J. Geophys. Res., 88*, 10831-10836, 1983a.

Dunkerton, T.J., Laterally-propagating Rossby waves in the easterly acceleration phase of the quasi-biennial oscillation. *Atmos.-Ocean, 21,* 55-68, 1983b.

Dunkerton, T.J., Annual variation of deseasonalized mean flow acceleration in the equatorial lower stratosphere. *J. Meteorol. Soc. Japan, 68,* 499-508, 1990.

Dunkerton, T.J. and D. Delisi, Climatology of the equatorial lower stratosphere. *J. Atmos. Sci., 42*, 1199-1208, 1985.

Dunkerton, T.J., and M.P.Baldwin, Quasi-biennial modulation of planetary - wave fluxes in the Northern Hemisphere winter, *J. Atmos. Sci., 48*, 1043-1061, 1991.

Fraedrich, K., S. Pawson and R. Wang, An EOF analysis of the vertical-time delay structure of the quasi-biennial oscillation. *J. Atmos. Sci., 50,* 3357-3365, 1993.

Geller, M.A., W. Shen, M. Zhang, W.-W. Tan, Calculations of the stratospheric quasi-biennial oscillation for time-varying wave forcing. *J. Atmos. Sci., 54*, 883-894, 1997.

Gray, W.M., Atlantic seasonal hurricane frequency, part I, El Nino and 30 mb quasi-biennial oscillation influences, *Mon. Weath. Rev., 112*, 1649-1668, 1984.

Gray, W.M., J.D. Scheaffer and J.A. Knaff, Hypothesized mechanism for stratospheric QBO influence on ENSO variability. *Geophys. Res. Lett., 19*, 107-110, 1992.

Hamilton, K., Dynamics of the Tropical Middle Atmosphere: A Tutorial Review. *Atmosphere-Ocean, 36,* 319-354, 1998a.

Hamilton, K., An imposed quasi-biennial oscillation in a comprehensive general circulation model: Response of the tropical and extratropical circulation. *J. Atmos. Sci., 55,* 2393-2418, 1998b.

Hamilton, K., R.J. Wilson and R. Hemler, Middle atmosphere simulated with high vertical and horizontal resolution versions of a GCM: Improvement in the cold pole bias and generation of a QBO-like oscillation in the tropics. *J. Atmos. Sci., 56*, 3829-3846, 1999.

Hamilton, K., R.J. Wilson and R. Hemler, Spontaneous stratospheric QBO-like oscillations

simulated by the GFDL SKYHI general circulation model. *J. Atmos. Sci., 58*, 3271-3292, 2001.

Holton, J.R. and H.-C. Tan, The influence of the equatorial quasi-biennial oscillation on the global circulation at 50 mb. *J. Atmos. Sci., 37*, 2200-2208, 1980.

Holton, J.R. and H.-C. Tan, The quasi-biennial oscillation in the Northern Hemisphere lower stratosphere. *J. Meteorol. Soc. Japan, 60*, 140-148, 1982.

Horinouchi, T. and S. Yoden, Wave-mean flow interaction associated with a QBO-like oscillation simulated in a simplified GCM. *J. Atmos. Sci., 55*, 502-526, 1998.

Hsieh, W. W., Nonlinear principal component analysis by neural networks, *Tellus, 53A,* 599-615, 2001.

Hsieh, W. W., and A. Wu, Nonlinear multichannel singular spectrum analysis of the tropical Pacific climate variability using a neural network approach. *Journal of Geophysical Research*, in press, 2002.

Kirby, M. J., and R. Miranda, Circular nodes in neural networks, *Neural Comp., 8,* 390-402, 1996.

Kramer, M. A., Nonlinear principal component analysis using autoassociative neural networks, *AIChE Journal, 37*, 233-243, 1991.

Marquardt, C. and B. Naujokat, An update of the equatorial QBO and its variability. *World Meteorological Organization Technical Document 814*, 87-90, 1997.

Monahan, A. H., Nonlinear principal component analysis: Tropical Indo-Pacific sea surface temperature and sea level pressure, *J. Climate, 14* , 219-233, 2001.

Naujokat, B., An update of the observed quasi-biennial oscillation of the stratospheric winds over the tropics. *J. Atmos. Sci., 43*, 1873-1877, 1986.

Quiroz, R.S., Period modulation of the stratospheric quasi-biennial oscillation. *Mon. Wea. Rev., 109*, 665-674, 1981.

Randel, W.J., J.F. Wu, J.M. Russell III, A. Roche and J. Waters, Seasonal cycles and QBO variations in stratospheric methane and water vapor observed in UARS HALOE data. *J. Atmos. Sci., 55*, 163-185, 1998.

Salby, M., and P. Callaghan, Connection between the Solar Cycle and the QBO: The Missing Link. *J. Clim., 13*, 2652-2662, 2000.

Takahashi, M., Simulation of the stratospheric quasi-biennial oscillation using a general circulation model. *Geophys. Res. Lett., 23*, 661-664, 1996.

Takahashi, M., The first realistic simulation of the stratospheric quasi-biennial oscillation in a general circulation model. *Geophys. Res. Lett., 26*, 1307-1310, 1999.

Tung, K.-K.. and H. Yang, Global QBO in circulation and ozone, part I, reexamination of

observational evidence. *J. Atmos. Sci. 51,* 2699-2707, 1994.

Wallace, J.M., The general circulation of the tropical lower stratosphere. *Rev. Geophys. Space Phys., 11*, 191-222, 1973.

Wallace, J.M., L. Panetta and J. Estberg, A phase-space representation of the equatorial stratospheric quasi-biennial oscillation. *J. Atmos. Sci., 50*, 1751-1762, 1993.

Wang, R., K. Fraedrich and S. Pawson, Phase-space characteristics of tropical stratospheric quasi-biennial oscillation. *J. Atmos. Sci., 52*, 4482-5000, 1995.

Xu, J.-S., On the relationship between the stratospheric quasi-biennial oscillation and the tropospheric Southern Oscillation. *J. Atmos. Sci., 49*, 725-734, 1992.

Table 1: The root mean square error (RMSE) (in ms^{-1}) between observations and the reconstructed component (RC) from NLPCA.cir mode 1 (NLRC1) as a function of the number of hidden neuron layers, m. Results are averaged for all 7 pressure levels.

m	RMSE
2	4.93
3	4.45
4	3.96
5	3.84
6	3.77
7	3.73
8	3.69

Table 2: The correlation and root mean square error (RMSE) (in ms^{-1}) between observations and the reconstructed component (RC) from NLPCA.cir mode 1 (NLRC1), from PCA mode 1 (RC1), and from PCA modes 1 and 2 (RC1+2). The last row gives the average over the 7 vertical levels.

pressure	correlation			RMSE		
(hPa)	NLRC1	RC1	RC1+2	NLRC1	RC1	RC1+2
10	0.966	0.840	0.953	4.91	10.27	5.75
15	0.978	0.983	0.984	4.12	3.62	3.54
20	0.983	0.924	0.977	3.56	7.47	4.20
30	0.985	0.512	0.972	3.07	15.27	4.17
40	0.979	0.086	0.973	3.26	15.76	3.64
50	0.958	0.469	0.934	3.76	11.59	4.71
70	0.851	0.780	0.822	3.44	4.10	3.73
average	0.957	0.656	0.945	3.73	9.73	4.25

Table 3: Indications of the phase of the tropical QBO in each January based on the NLPCA and based on the linear PCA. Also given is the anomaly in the January-mean 40 hPa zonal wind, u. "W" means westerly (i.e. eastward or positive) zonal wind phase. Results shown for 1956-2000, although the analysis to define the E and W phase ranges in the NLPCA and linear PCA were defined on the basis of 1958-1999 data only.

Year	NLPCA phase	40 hPa u m-s^{-1}	PCA phase	Year	NLPCA phase	40 hPa u m-s^{-1}	PCA phase
1956	W	8.3	W	1980	E	-21.9	E
1957	E	-24.3	E	1981	W	16.5	W
1958	W	13.6	W	1982	E	-12.4	E
1959	E	-19.4	E	1983	W	18.1	W
1960	W	5.6	W	1984	E	-6.3	E
1961	E	-20.6	E	1985	E	-4.0	E
1962	W	13.2	W	1986	W	17.8	W
1963	E	-19.7	E	1987	E	-6.0	E
1964	W	6.6	W	1988	W	11.7	W
1965	W	13.8	W	1989	W	14.4	W
1966	E	-27.5	E	1990	E	-26.7	E
1967	W	17.1	W	1991	W	12.6	W
1968	E	6.6	E	1992	E	-13.4	E
1969	E	-26.8	E	1993	W	16.0	W
1970	W	11.8	W	1994	E	-0.4	E
1971	E	-26.6	E	1995	E	15.9	W
1972	W	15.4	W	1996	W	5.1	E
1973	E	-17.9	E	1997	E	-21.3	E
1974	W	13.1	W	1998	W	16.4	W
1975	E	-18.4	E	1999	E	-4.3	E
1976	W	16.4	W	2000	W	15.3	W
1977	E	-10.4	E				
1978	W	14.6	W				
1979	W	13.6	W				

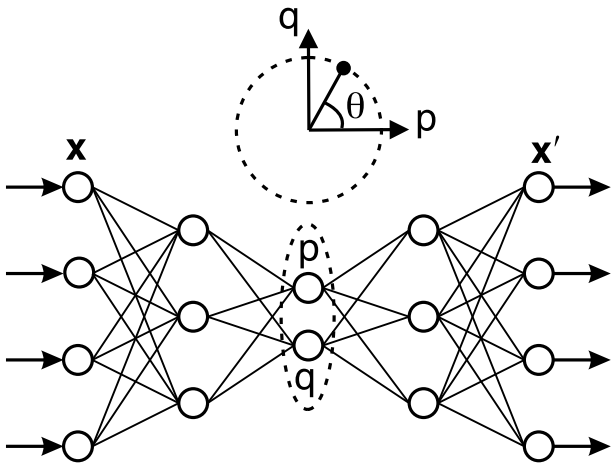

Figure 1: A schematic diagram illustrating the NN model for calculating the NLPCA with a circular node at the bottleneck (NLPCA.cir). The model is a standard feedforward NN (i.e. multi-layer perceptron), with 3 'hidden' layers of variables or 'neurons' (denoted by circles) sandwiched between the input layer $\mathbf{x}$ on the left and the output layer $\mathbf{x}'$ on the right. Next to the input layer (with l neurons) is the encoding layer (with m neurons), followed by the 'bottleneck' layer, then the decoding layer (with m neurons), and finally the output layer (with l neurons), i.e. a total of 4 layers of transfer functions are needed to map from the inputs to the outputs. A neuron v_i at the ith layer receives its value from the neurons $\mathbf{v}_{i-1}$ in the preceding layer, i.e. $v_i = f_i(\mathbf{w}_i \cdot \mathbf{v}_{i-1} + b)$, where $\mathbf{w}_i$ is a vector of weight parameters and b a bias parameter, and the transfer functions f_1 and f_3 are the hyperbolic tangent functions, while f_2 and f_4 are simply the identity functions. In NLPCA.cir, the bottleneck contains two neurons p and q confined to lie on a unit circle, i.e. only 1 degree of freedom as represented by the angle θ. Effectively, a nonlinear function $\theta = F(\mathbf{x})$ maps from the higher dimension input space to the lower dimension bottleneck space, followed by an inverse transform $\mathbf{x}' = G(\theta)$ mapping from the bottleneck space back to the original space, as represented by the outputs. To make the outputs as close to the inputs as possible, the cost function $J = \langle \|\mathbf{x} - \mathbf{x}'\|^2 \rangle$ (i.e. the mean square error, MSE) is minimized (where $\langle \cdots \rangle$ denotes a sample or time mean). Through the optimization, the values of the weight and bias parameters are solved. Data compression is achieved by the bottleneck, yielding the nonlinear principal component (NLPC) θ. In our application, there are 7 inputs and 7 outputs, as the wind data are available at 7 vertical levels.

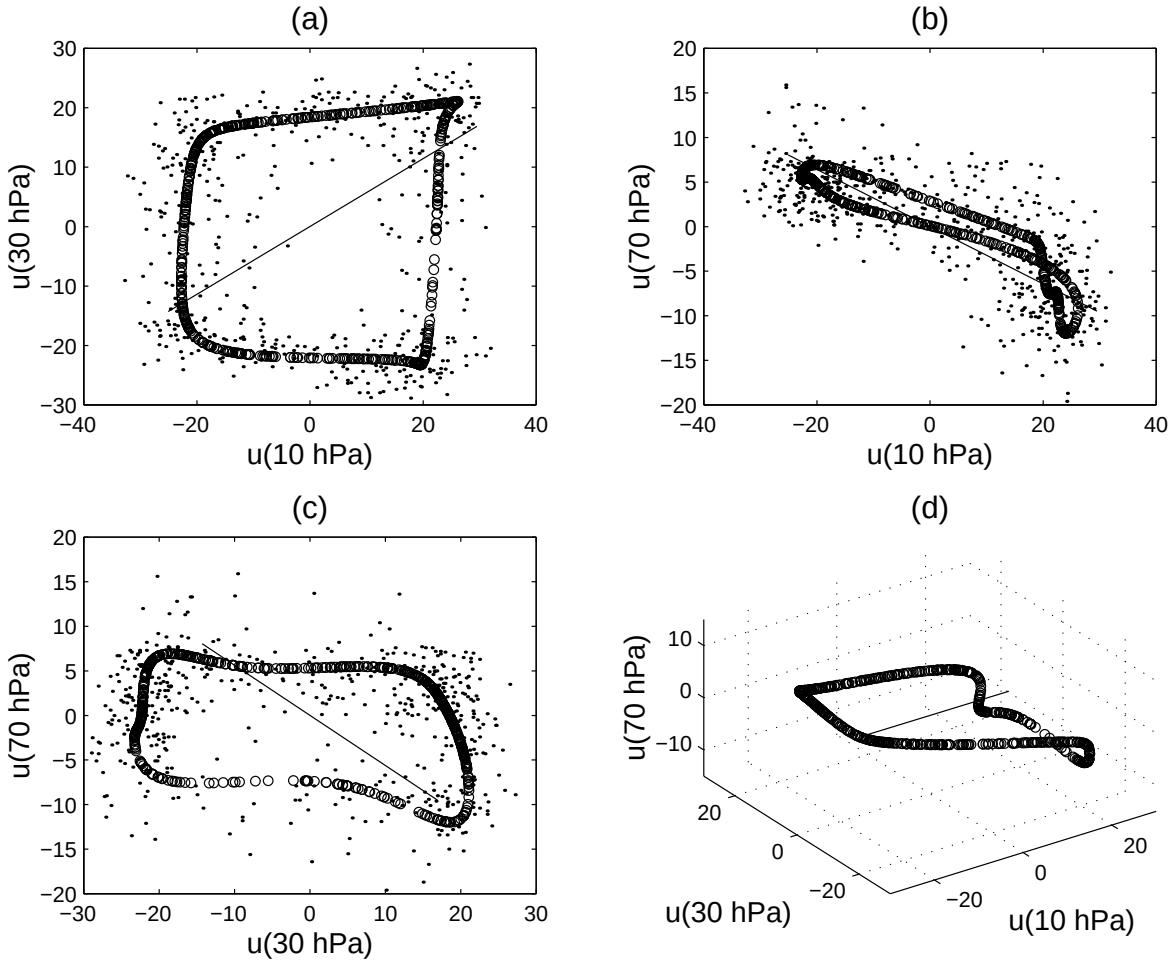

Figure 2: The NLPCA.cir mode 1 solution is shown by the (overlapping) circles, while the data are shown as dots. For comparison, the PCA mode 1 solution is shown as a thin straight line. Only 3 out of 7 dimensions are shown, namely u at the top, middle and bottom levels (10, 30 and 70 hPa). Panels (a)-(c) give 2-D views, while (d) gives a 3-D view.

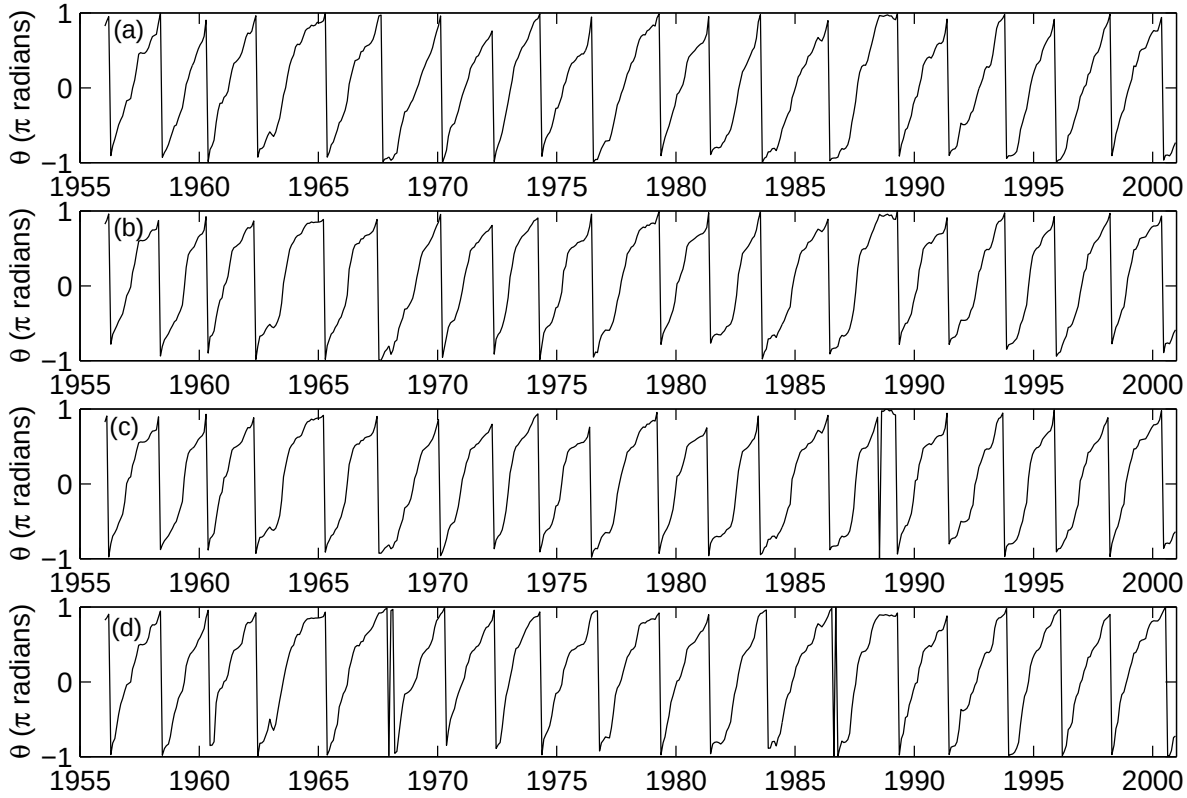

Figure 3: The mode 1 nonlinear principal component θ time series for (a) $m = 2$, (b) $m = 4$, (c) $m = 6$ (the chosen solution), and (d) $m = 8$, where m is the number of hidden neurons in the encoding layer. Note θ (plotted in π radians) is a cyclic variable bounded between $[-1, 1]$. The values of θ in panels (a), (b) and (d) have each been adjusted by a constant value, so θ in all panels have the same starting value.

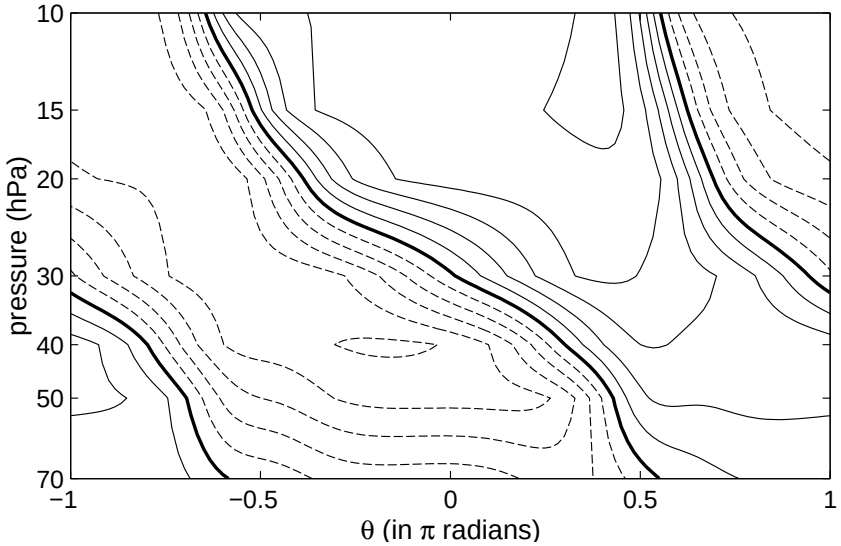

Figure 4: Contour plot of the NLPCA.cir mode 1 zonal wind anomalies as a function of pressure and θ. Contour interval is 5 ms^{-1}, with positive contours (i.e. westerly or eastward winds) indicated by solid lines, negative contours by dashed lines, and zero contours by thick lines.

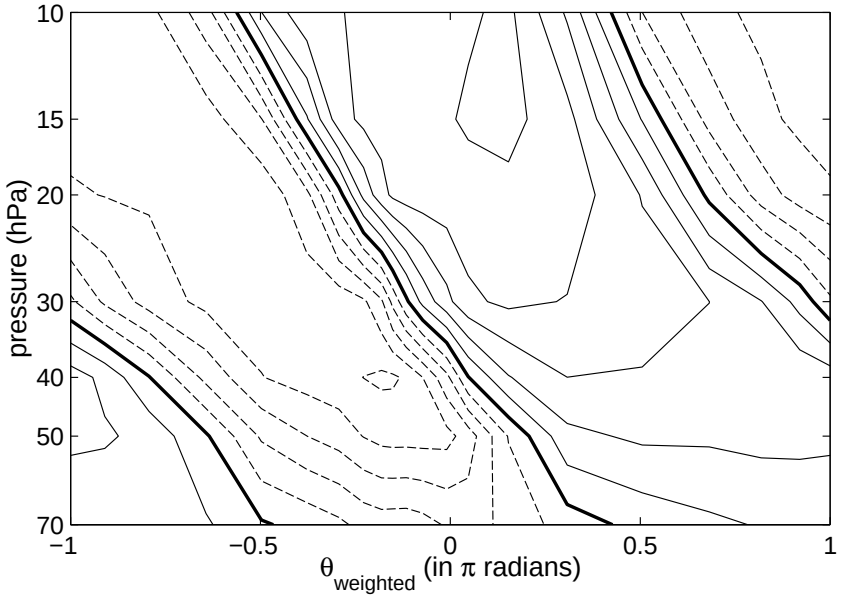

Figure 5: Contour plot of the NLPCA.cir mode 1 zonal wind anomalies as a function of pressure and θ_{weighted}, where θ_{weighted} is more representative of actual time during a cycle than θ. Contour interval is 5 ms^{-1}.

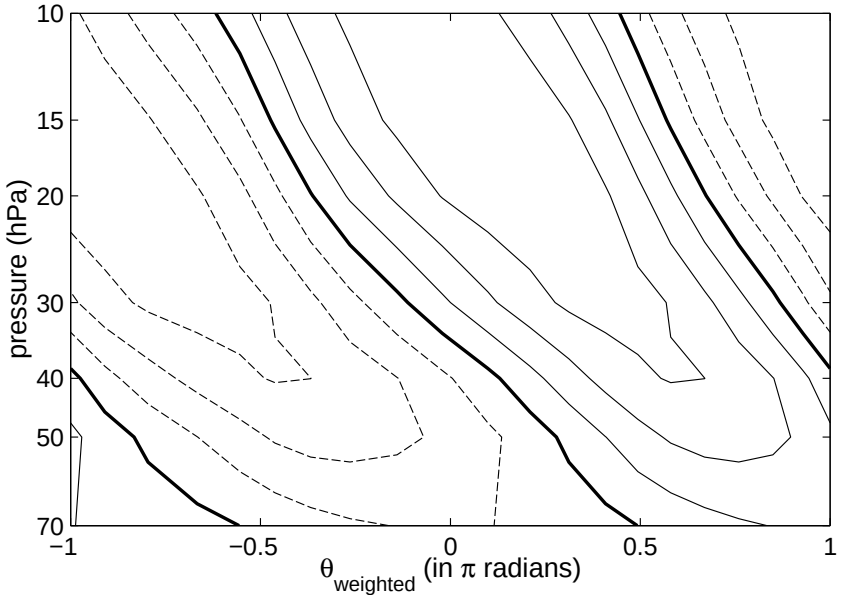

Figure 6: As in Fig. 5, but for the equivalent analysis using a linear circular approach.

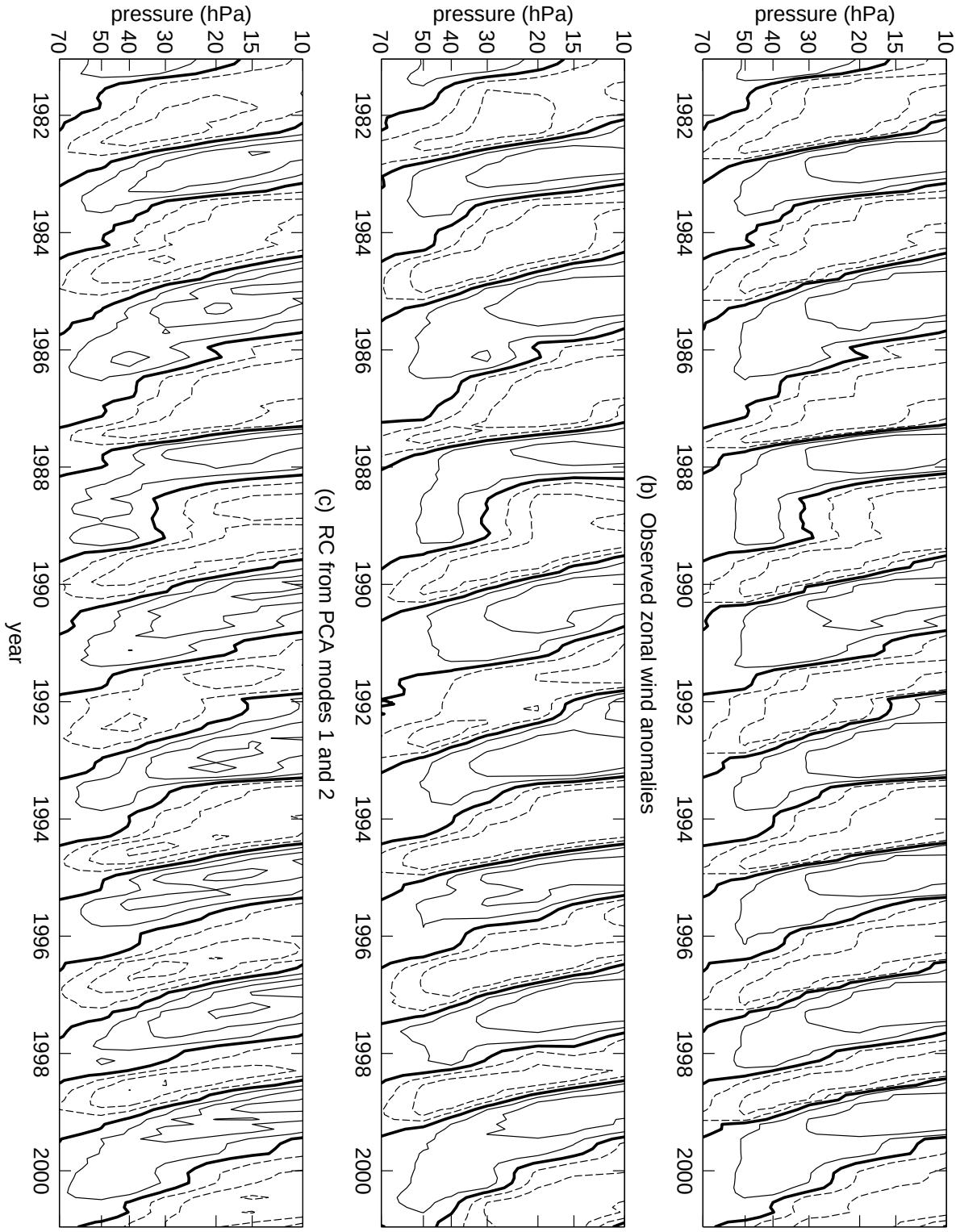

Figure 7: (a) The reconstructed component (RC) from NLPCA.cir mode 1, (b) the observed zonal wind anomalies, and (c) the RC from the PCA modes 1 and 2. Only the period 1981-2000 is shown. The observed anomalies in (b) were smoothed by a 3-month running mean for better legibility. Negative contours are dashed, while the zero contour is thickened. Contour intervals are 10 ms^{-1}.

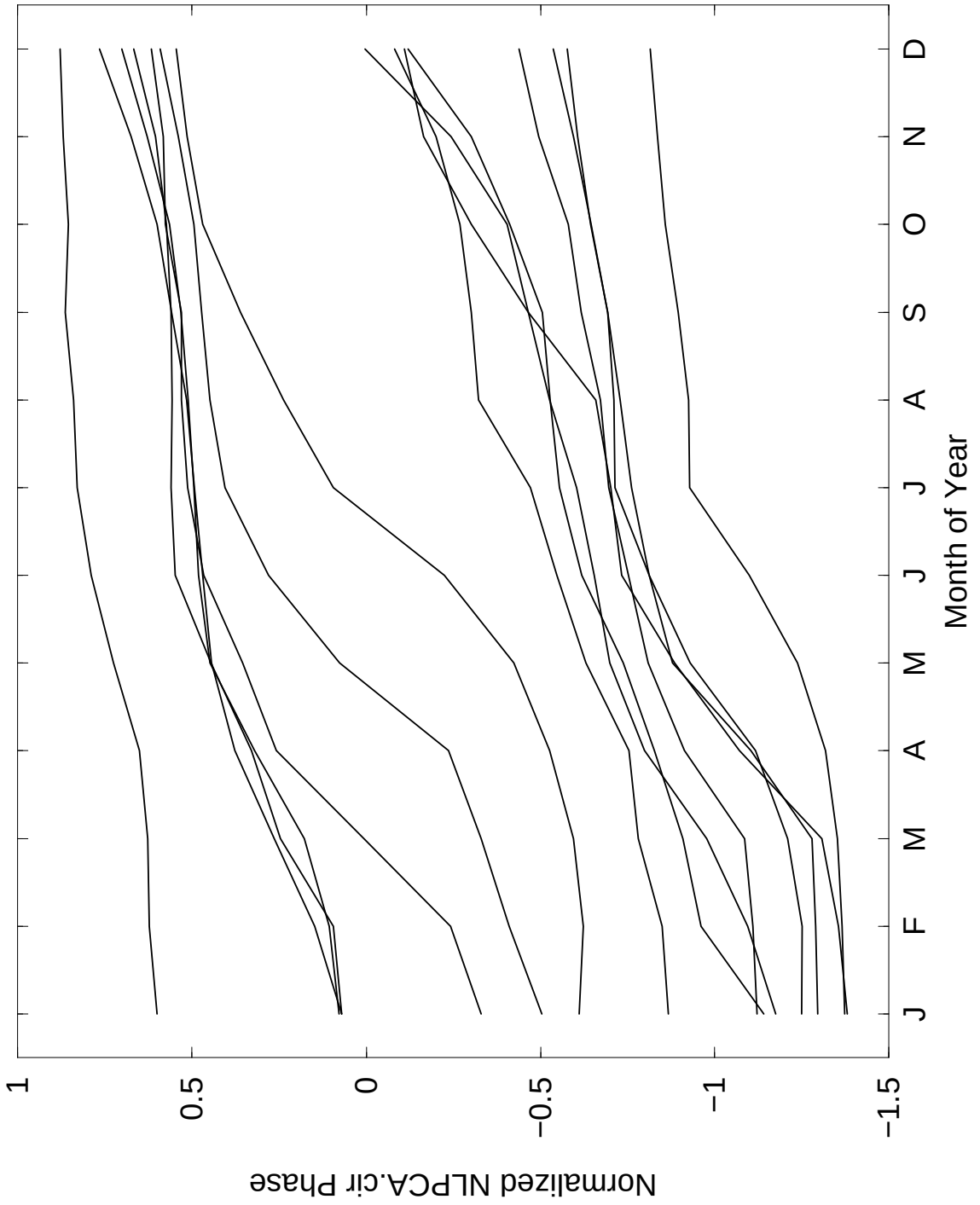

Figure 8: The NLPCA.cir phase, θ, in each month of the year for each year from 1956-1970. The phases are normalized by π and are plotted modulo 2π in a way to show the phase progression continuously each year.

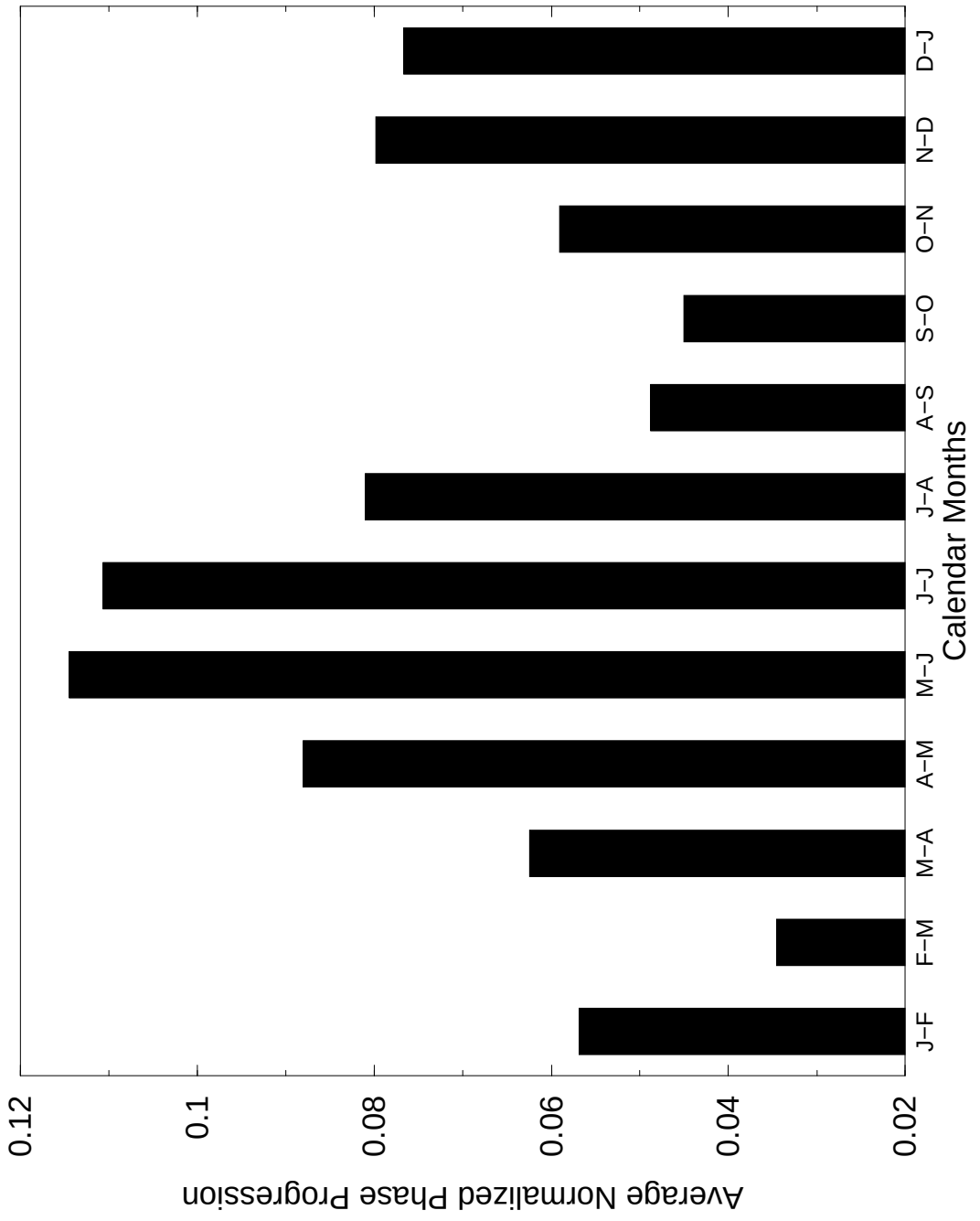

Figure 9: The average QBO phase progression between successive months for January-to-February (J-F), February-to-March (F-M), ... through December-to-January (D-J).

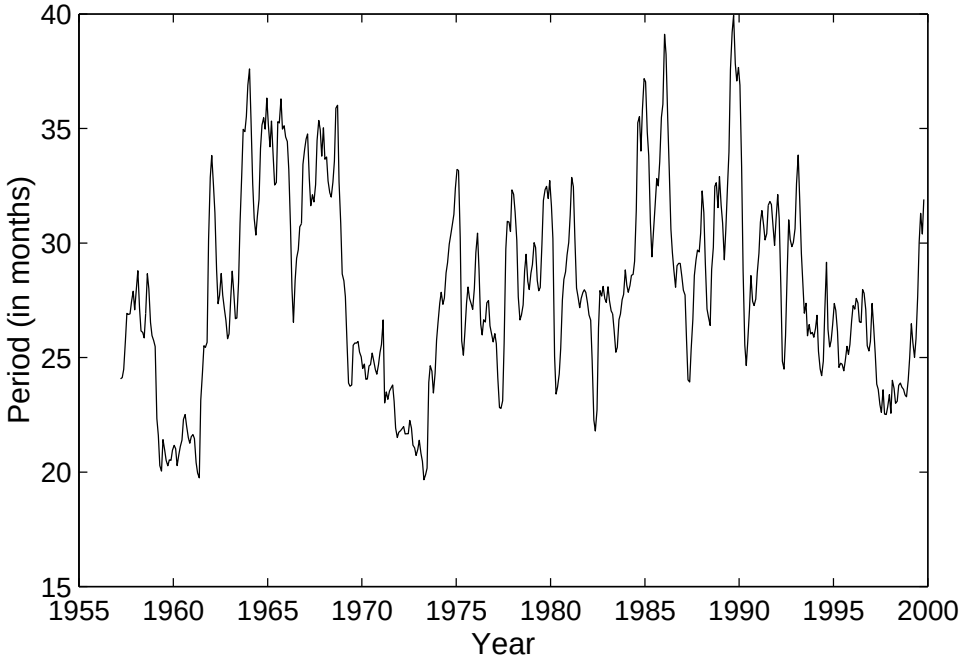

Figure 10: Period of the QBO as a function of time. The period was estimated from $2\pi/\langle\Delta\theta/\Delta t\rangle$, where $\langle\ldots\rangle$ denotes averaging over 28 months.